SUPPLEMENTARY DATA

Supplementary Figure 1. CDCP1 overexpression correlate with PTEN loss in human CRPC and metastasis

(**A**) Percentage of CDCP1 positive samples in normal prostate/benign, localized HSPC, primary CRPC, advanced/metastatic PCa and distant metastases in human prostate cancers TMA2 (n=438). (**B**) Left panel, Representative IHC images of CDCP1 protein detection in the biopsy of hormone-sensitive prostate cancer (HSPC) and castration-resistant prostate cancer (CRPC) in the same patient. Scale bars represent 50 μm. Right panel, Expression (H-score) of membranous CDCP1 in matched biopsies at HSPC and CRPC stage in 26 prostate cancer patients. Median H-scores and interquartile range are shown. P-values were calculated using the Wilcoxon matched-pair signed-rank test. (**C**) Scattered plots are showing the correlation between PTEN and CDCP1 mRNA levels in human prostate tumors in the indicated datasets. (**D**) Table with the results of the correlation analysis between PTEN and CDCP1 and expression in normal and all tumors (primary tumor and metastatic) specimens from the indicated datasets. (**E**) Anti-correlation between CDCP1 mRNA expression levels and its promoter methylation levels in TCGA dataset. (**F**) Association between CDCP1 expression levels, its promoter methylation and PTEN deletion/mutation in TCGA dataset. (**G**) Disease-free survival of TCGA dataset patients based on CDCP1mRNA expression levels (cpm).

Supplementary Figure 2. Generation of the hCDCP1 prostate conditional mouse model

(**A**) Schematic description of engineering the LoxP elements and the stop element allowing the prostate-specific expression of human CDCP1 after Cre expression under the control of a Probasin promoter. (**B**) Left panel, PCR-based identification of the CDCP1-transgene element in WT ES cells and three targeted ES cell clones. Right panel, Southern blot analysis of SpeI digested genomic DNA of WT ES and three targeted ES cell clones hybridized with the internal probe. (**C**) Representative IHC images of CDCP1 staining in anterior prostates (AP) in *CDCP1* and WT mice. Scale bar represents 500 μm and 250 mm for upper and lower panel respectively. (**D**) qRT-PCR PCR analysis of CDCP1 in anterior prostate (AP), ventral prostate (VP) and dorsal-lateral prostate (DLP) of 12 weeks old mice (n=3). (**E**) Western blot analysis of CDCP1 protein level in AP, VP and DLP of 12 weeks old WT and *CDCP1* mice. (**F**) Left panel, Western blot analysis of CDCP1 expression in different prostate cancer cell lines, Patient-derived xenografts and our transgenic mouse model prostate. Right panel, Quantification of fold change in CDCP1 protein levels in the indicated samples. (**G**) Representative images of H&E staining of AP, VP and DLP of 12 months old WT and *CDCP1* mice. Scale bar represents 500 μm.

Supplementary Figure 3. Generation of the Drosophila melanogaster model overexpressing both a wild type (CDCP1-WT) and a mutant (CDCP1-delta) form of hCDCP1

(**A**) Western blot analysis of indicated proteins in the salivary glands expressing hCDCP1-WT or hCDCP1-delta driven by ptc-gal4 and LacZ Control. (**B**) Representative immunofluorescent images of CDCP1 and E-Cadherin expression in salivary glands of the indicated genotypes. Scale bar represents 100 mm length. (**C**) Representative images of extra machrochaetae formation in adult fly notum expressing hCDCP1-WT or hCDCP1-delta or LacZ Control. Scale bar represents 100 mm length. (**D**) Representative images of macrochaetae formation in adult fly notum in heterozygous Src kinase mutant animals (src42A$^{+/-}$; src64B$^{+/-}$) or heterozygous Src kinase mutant animals are expressing hCDCP1-WT (src42A$^{+/-}$; src64B$^{+/-}$, CDCP1-WT). Scale bar represents 100 mm length.

Supplementary Figure 4. CDCP1 overexpression in Pten-null tumors promotes a metastatic phenotype.

(**A**) Representative immunofluorescence staining of Keratin8, Keratin5, E-Cadherin and DAPI in lumbar lymph nodes from 10 months old *CDCP1; Ptenpc*$^{-/-}$ mice. Insets represent higher magnification (scale bar 50 μm) (n=4/8). Scale bar represents 5 mm length. (**B**) Representative images of H&E, PanK, CDCP1 and AR staining in lungs from 10 months old *CDCP1; Pten*$^{pc-/-}$ mice (n=1/10). Scale bar represents 5 mm length. (**C**) Growth curve estimated by crystal violet staining in WT, *CDCP1, Pten*$^{-/-}$ and *CDCP1; Pten*$^{-/-}$ MEFs (n=3). (**D**) Left panel, Representatives images of the trans-well migration assay in WT, *CDCP1, Pten*$^{-/-}$ and *CDCP1; Pten*$^{-/-}$ MEFs. Scale bar represents 5 mm length. Right panel, quantification of the migrated cells (n=3). Error bars indicate standard deviation (SD). *P<0.05. Statistic test used: two-tailed t-test.

Supplementary Figure 5. CDCP1 overexpression in Pten-loss context leads to castration-resistant prostate cancer

(A) Upper panel, representative images of anterior prostate of *Pten*$^{pc-/-}$ and *CDCP1; Pten*$^{pc-/-}$ non-castrated and castrated animals. Scale 1 cm. Lower panel, Quantification of anterior prostate weights and volume of *Pten*$^{pc-/-}$ and *CDCP1; Pten*$^{pc-/-}$ castrated and non-castrated mice (n=4). (**B**) Representatives images of H&E staining of *Pten*$^{pc-/-}$ and *CDCP1; Pten*$^{pc-/-}$ anterior prostate of non-castrated and castrated mice. All mice were sacrificed at the age of 20 weeks, 8 weeks after castration. Scale bar represents 5 mm length. (**C**) Quantification of histopathological markers from anterior prostate tissue of the indicated genotypes of *Pten*$^{pc-/-}$ and *CDCP1; Pten*$^{pc-/-}$ castrated and non-castrated mice (n=3). (**D**) Left panel, Representatives images of KI67 staining of *Pten*$^{pc-/-}$ and *CDCP1; Pten*$^{pc-/-}$

anterior prostate of non-castrated and castrated mice. Scale bar represents 5 mm length. Right panel, Quantification of Ki-67 staining in *Pten*$^{pc-/-}$ and *CDCP1; Pten*$^{pc-/-}$ anterior prostate of non-castrated and castrated mice at 20 weeks of age (n=3-4). (**E**) Western blot analysis and protein fold change quantification of indicated protein in the anterior prostate of *Pten*$^{pc-/-}$ and *CDCP1; Pten*$^{pc-/-}$ castrated mice at 20 weeks of age. (**F**) c-Myc relative expression fold change in *Pten*$^{pc-/-}$ and *CDCP1; Pten*$^{pc-/-}$ castrated mice. (**G**) Representative image of IHC staining of c-Myc and p-AKT (s473) in *Pten*$^{pc-/-}$ and *CDCP1; Pten*$^{pc-/-}$ castrated mice. Scale bar represents 200 µm. (**H**) Western blot analysis of CDCP1, c-Myc, p-Src, Src, p-Erk1/2 and Erk1/2 in TRAMP-C1-GFP and TRAMP-C1-CDCP1 mouse prostate cancer cell lines. (**I**) Left panel, representative scheme of TRAMP-C1 allograft experiment. Middle panel, Allograft tumors volume (mm^3) of TRAMP-C1-GFP and TRAMP-C1-CDCP1 cells. (n=5 in both groups). Right panel, Percentage of cumulative survival of TRAMP-C1-GFP and TRAMP-C1-CDCP1 allografts. Error bars indicate standard deviation (SD). **P<0.01; ***P<0.001. Statistic test used: two-tailed t-test for panel A, D, E and F. log-rank (mantel-cox) test for panel I.

Supplementary Figure 6. CDCP1 overexpression promotes the escape from senescence in MEFs

(**A**) Representative images and quantification of SA-β-Gal staining in WT, *CDCP1, Pten*$^{-/-}$ and *CDCP1; Pten*$^{-/-}$ MEFs (n=3). Scale bar represents 5 mm length. (**B**) Western blot analysis of indicated proteins in WT, CDCP1, *Pten*$^{-/-}$ and *CDCP1; Pten*$^{-/-}$ MEFs. (**C**) Protein fold change quantification of COUP-TFII and Cyclin D1. (**D**) Quantitative real-time PCR analysis of c-Myc, Cyclin D1 and COUP-TF-II expression in *Pten*$^{-/-}$ and *CDCP1; Pten*$^{-/-}$ MEFs treated with saracatinib (100 nM) for 12 h (n=4). (**E**) Quantification of SA-β-Gal positive cells in *Pten*$^{-/-}$ and *CDCP1; Pten*$^{-/-}$ MEFs treated with saracatinib (100 nM) and DMSO for 12h. (**F**) Quantitative real-time PCR analysis of c-Myc, Cyclin D1 and COUP-TF-II expression in *Pten*$^{-/-}$ and *CDCP1; Pten*$^{-/-}$ MEFs transfected with si-c-Myc and control si-Ctrl after 48h (n=5). (**G**) Quantification of senescence-associated β-Gal (SA-β-Gal) staining in *Pten*$^{-/-}$ and *CDCP1; Pten*$^{-/-}$ MEFs transfected with si-c-Myc and control si-Ctrl after 48h (n=4). (**H**) Schematic representation showing the transcription-starting site of COUP-TFII and c-Myc binding site (http://www.sabiosciences.com). Error bars indicate standard deviation (SD) for panel A, D, E, F and G and standard error mean (SEM) for panel C. *P<0.05; **P<0.01; ****P<0.0001. The following statistical test were used: two-tailed t-test for panels A, D, E, F and G and one-tailed t-test for panel C.

Supplementary Figure 7. CDCP1 overexpression promotes escape from senescence in human prostate cancer cell lines

(**A**) Western blot analysis of the CDCP1 protein in infected PC3 cells expressing PLKO-sh-CDCP1 (sh-CDCP1#1) and doxycycline-inducible Tripz-sh-CDCP1 (sh-CDCP1#2). (**B**) Quantification of in

vitro 3D growth of CDCP1 depleted PC3 cells and control as measured by Luminescent Cell Viability Assay (n=4). (**C**) Representative image of SA-β-Gal staining of CDCP1 depleted PC3 cells and control PC3. Scale bar represents 5 mm length. (**D**) Bar graph represents the percentage of SA-β-Gal positive cells in all groups (n=3). (**E**) Left panel, Xenograft tumor growth (cm^3) of PC3 cells expressing doxycycline-inducible shRNA-control (sh-Ctrl#2) and shRNA-CDCP1 (sh-CDCP1#2). Insets represent PC3 xenograft tumors for both groups. Scale 1 cm. Right panel, bar graph represents tumor weight in both groups (n=4). (**F**) qRT-PCR of p27 and p21 mRNA levels in PC3 sh-Ctrl#2 and PC3 sh-CDCP1#2 xenografts tumors (n=4). (**G**) Western blot analysis of CDCP1, p-SRC, SRC, c-MYC, CYCLIN D1, COUP-TFII in PC3 sh-Ctrl#2 and PC3 sh-CDCP1#2 xenografts tumor. (**H**) Western blot analysis of CDCP1 and c-MYC in androgen deprivation sensitive LNCaP (LNCaP-parental) and androgen deprivation insensitive LNCaP-abl human prostate cancer cell line. (**I**) Left panel, Western blot analysis of CDCP1 and c-MYC in LNCaP-abl-shCtrl#2 and LNCaP-sh-CDCP1#2. Right panel, Fold change in growth of LNCaP-abl-shCtrl#2 and LNCaP-sh-CDCP1#2 (n=3). (**J**) Left panel, Representative images of SA-β-Gal staining in LNCaP-abl expression sh-Ctrl#2 and sh-CDCP1#2. Scale bar represents 5 mm length. Right panel, bar graph represents the percentage of SA-β-Gal positive cells in LNCaP-abl expression sh-Ctrl#2 and sh-CDCP1#2. (n=3). Error bars indicate standard deviation (SD). *P<0.05; **P<0.01; ***P<0.001. Statistic test used: two- tailed t-test.

Supplementary Figure 8. CDCP1 expression regulated by AR activity

(**A**) Left panel, negative correlation between CDCP1 expression levels and AR expression levels in the cases with PTEN expression low. Right panel, negative correlation between CDCP1 expression levels and AR expression levels in the cases with AR gene copy number normal. (**B**) Negative correlation between mRNA expression levels of CDCP1 with AR pathway activity (single sample GSEA score). (**C**) Dot-plots are showing FDG staining in LNCaP cells untreated, LNCaP ADS and ADI. (**D**) Quantitative real-time PCR analysis of CDCP1 mRNA levels in PC3 and PC3-AR kept in full media, in FAD or under DHT stimulation. (**E**) Western blot analysis of CDCP1 and PTEN in androgen insensitive human prostate cancer cell lines (22RV1 and PC3) (n=3). (**F**) Left panel, Western blot analysis of CDCP1, AR, p-AKT and AKT in 22RV1 treated with PI3K inhibitor in normal condition and in FAD. Right panel, Quantification of fold change in CDCP1 protein levels in 22RV1 untreated or treated with PI3K inhibitor in normal condition and in FAD (n=3). (**G**) Left panel, Quantification of fold change in growth by crystal violet in LNCaP kept in full media and FAD and treated with and without the mAb-CUB4. Right panel, SA-β-Gal staining in cells treated with the indicated antibody. Scale bar represents 50 μm. (**H**) Western blot analysis of CDCP1 expression and

p-SRC in LNCaP xenografts groups. Error bars indicate standard deviation (SD). **P<0.01; ***P<0.001. Statistic test used: two- tailed t-test.

A

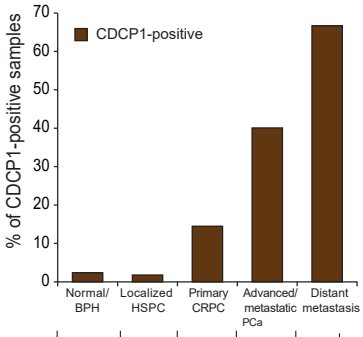

	Normal/ BPH	Localized HSPC	Primary CRPC	Advanced/ metastatic PCa	Distant metastasis
Total	43	115	79	192	6
CDCP1-positive	1	2	10	77	4

B

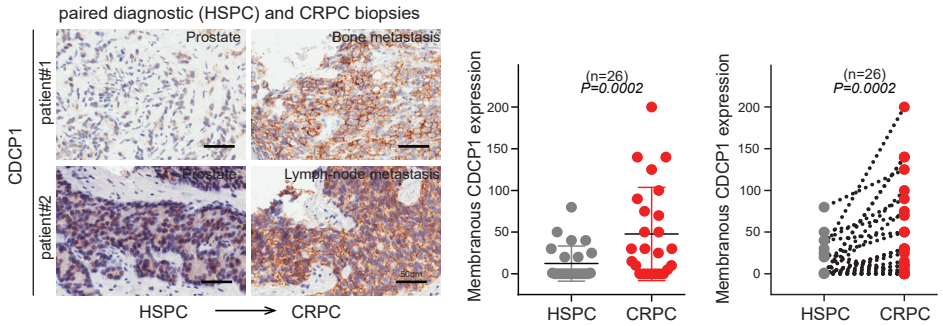

C

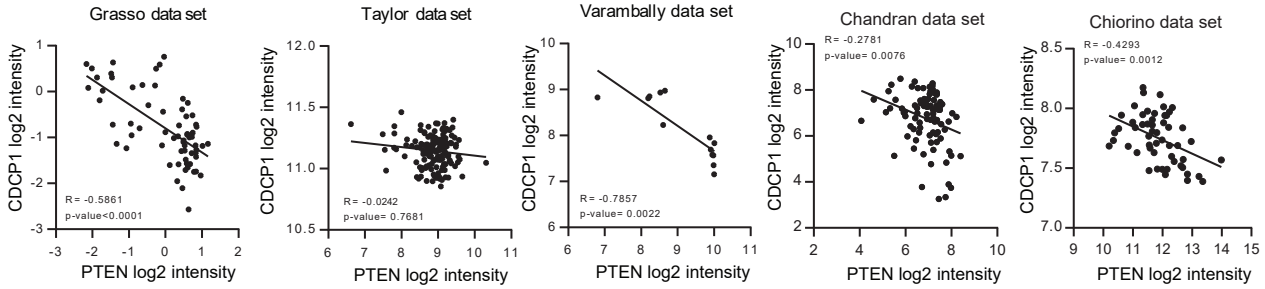

D

data set	anti-correlation	tissue type	R	p-value
Grasso	not significant	Normal	-0.119	0.716
	significant	all tumours	-0.5861	<0.0001
Taylor	not significant	Normal	0.298	0.117
	not significant	all tumours	-0.024	0.7681
Varambally	not significant	Normal	-0.086	0.919
	significant	all tumours	-0.7857	0.0022
Chandran	not significant	Normal	-0.1735	0.134
	significant	all tumours	-0.2781	0.0076
Chiorino	not significant	Normal	-.3582	0.2090
	significant	Tumours	-0.4293	0.0012

E

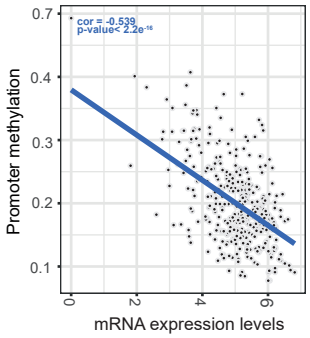

F

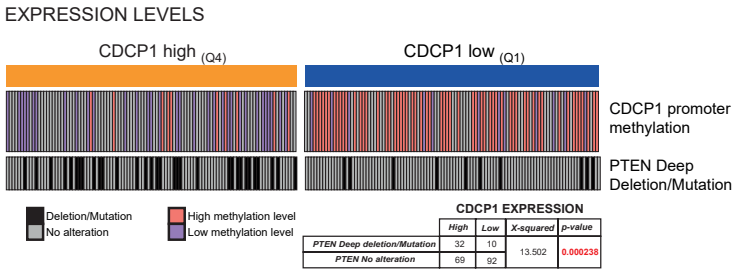

CDCP1 EXPRESSION

	High	Low	X-squared	p-value
PTEN Deep deletion/Mutation	32	10	13.502	0.000238
PTEN No alteration	69	92		

G

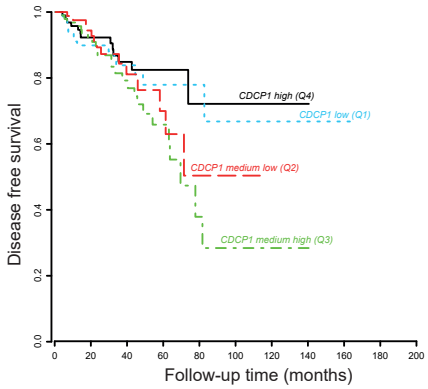

Supplementary Figure 1. CDCP1 overexpression correlate with PTEN loss in human CRPC and metastasis
(A) Percentage of CDCP1 positive samples in normal prostate/benign, localized HSPC, primary CRPC, advanced/metastatic PCa and distant metastases in human prostate cancers TMA2 (n=438). (B) Left panel, Representative IHC images of CDCP1 protein detection in the biopsy of hormone-sensitive prostate cancer (HSPC) and castration-resistant prostate cancer (CRPC) in the same patient. Scale bar represent 50 µm. Right panel, Expression (H-score) of membranous CDCP1 in matched biopsies at HSPC and CRPC stage in 26 prostate cancer patients. Median H-scores and interquartile range are shown. P-values were calculated using the Wilcoxon matched-pair signed-rank test. (C) Scattered plots are showing the correlation between PTEN and CDCP1 mRNA levels in human prostate tumors in the indicated datasets. (D) Table with the results of the correlation analysis between PTEN and CDCP1 and expression in normal and all tumors (primary tumor and metastatic) specimens from the indicated datasets. (E) Anti-correlation between CDCP1 mRNA expression levels and its promotermethylation levels in TCGA dataset. (F) Association between CDCP1 expression levels, its promoter methylation and PTEN deletion/mutation in TCGA dataset. (G) Disease-free survival of TCGA dataset patients based on CDCP1mRNA expression levels (cpm).

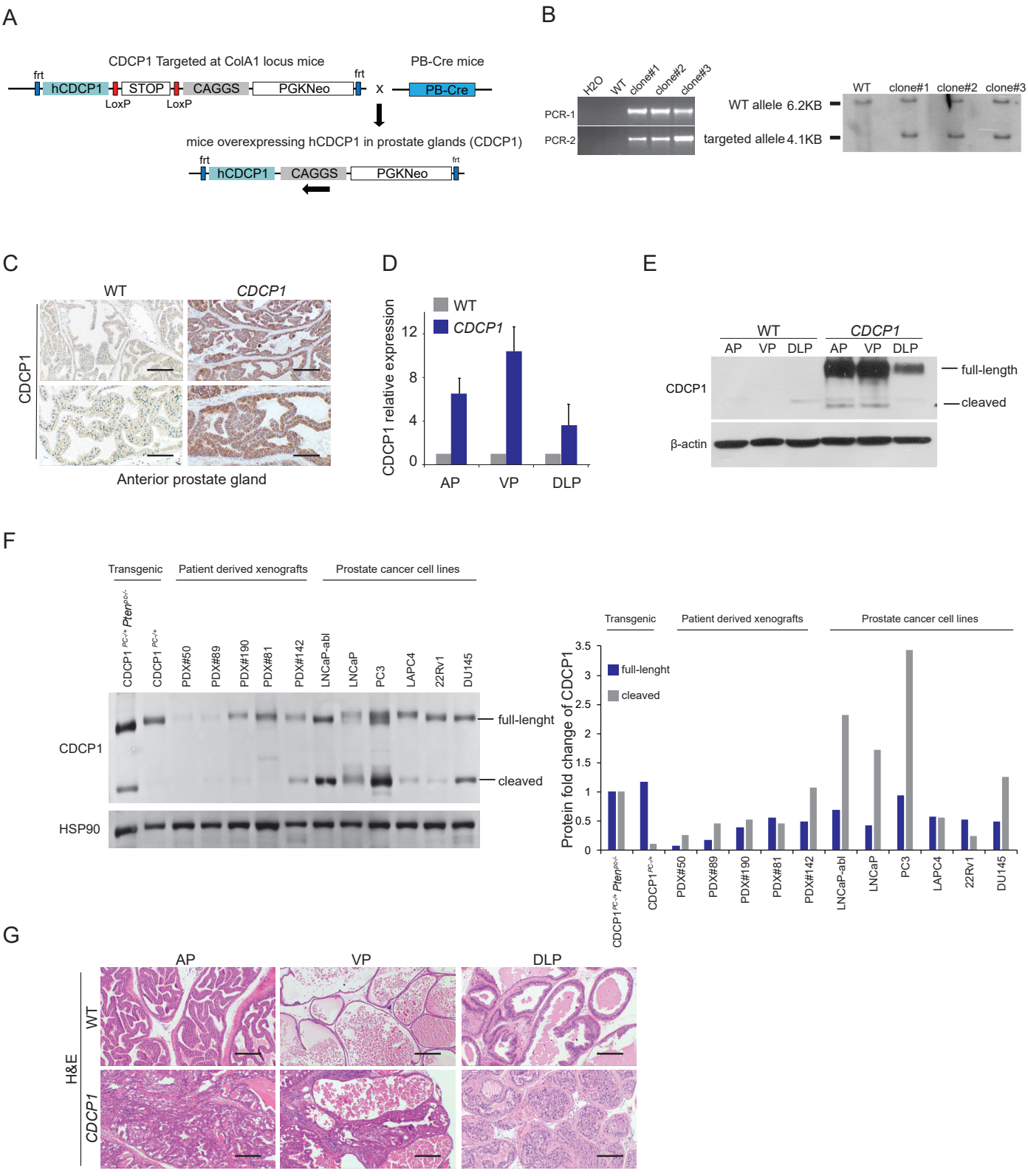

Supplementary Figure 2. Generation of the hCDCP1 prostate conditional mouse model

(A) Schematic description of engineering the LoxP elements and the stop element allowing the prostate-specific expression of human CDCP1 after Cre expression under the control of a Probasin promoter. (B) Left panel, PCR-based identificaiton of CDCP1-transgene element in WT ES cell clones. Right panel, Southern blot analysis of SpeI digested genomic DNAof WT ES and three targeted ES cell clones hybridized with the internal probe. (C) Representative IHC images of CDCP1 staining in anterior prostates (AP) in CDCP1 and WT mice.Scale bar represents 500 μm and 250 mm for upper and lower panel respectively . (D) qRT-PCR analysis of CDCP1 in anterior prostate (AP), ventral prostate (VP) and dorsal-lateral prostate (DLP) of 12 weeks old mice (n=3). (E) Western blot analysis of CDCP1 protein levels in AP, VP and DLP of 12 weeks old WT and CDCP1 mice. (F) Left panel, Western blot analysis of CDCP1 expression in different prostate cancer cell lines, Patient-derived xenografts and our transgenic mouse model prostate. Right panel, Quantification of fold change in CDCP1 protein levels in the indicated samples. (G) Representative images of H&E stainings of AP, VP and DLP of 12 months old WT and CDCP1 mice. Scale bar represents 500 μm.

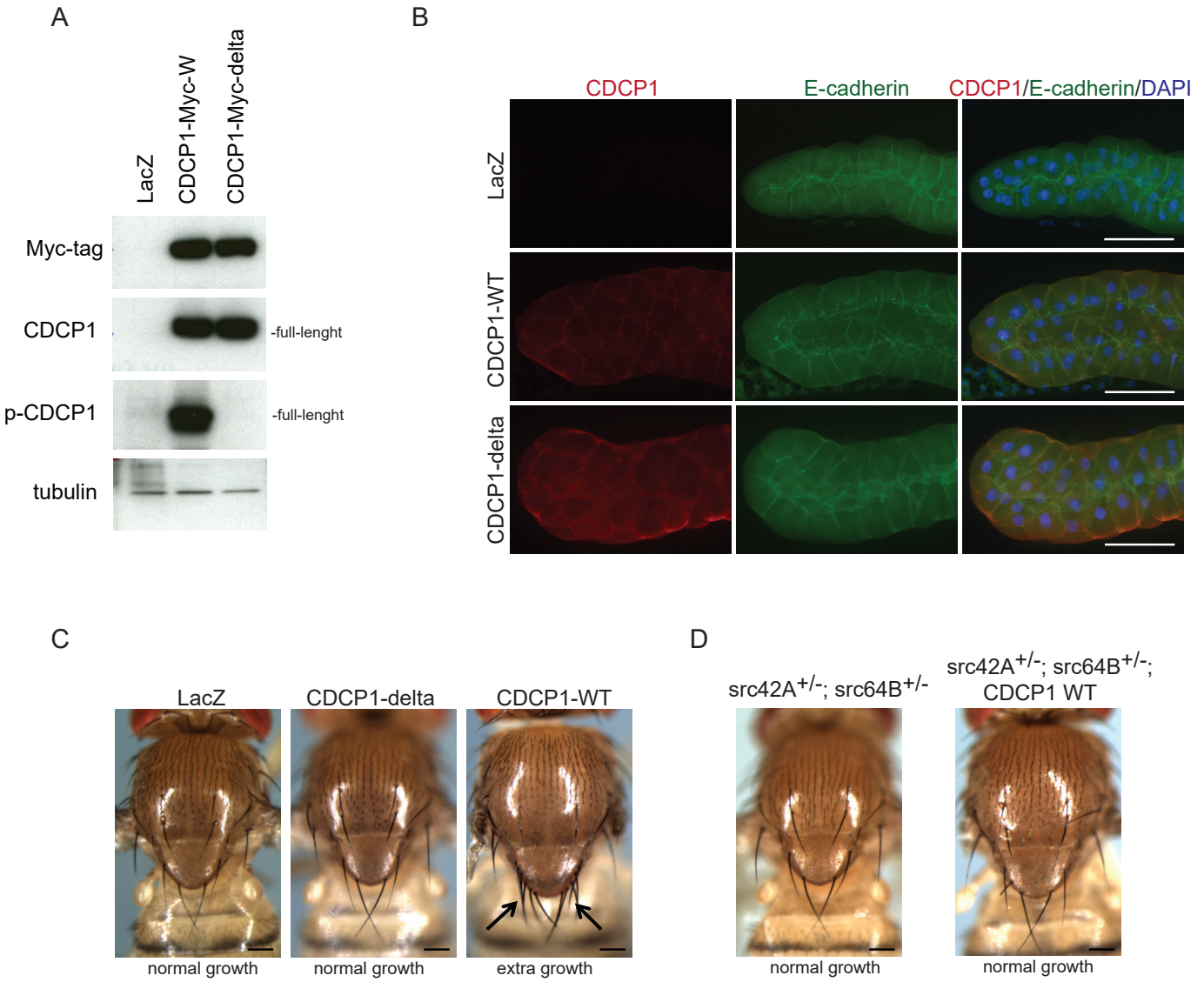

Supplementary Figure 3. Generation of the Drosophila melanogaster model overexpressing both a wild type (CDCP1-WT) and a mutant (CDCP1-delta) form of hCDCP1

(A) Western blot analysis of indicated proteins in the salivary glands expressing hCDCP1-WT or hCDCP1-delta driven by ptc-gal4 and LacZ Control. (B) Representative immunofluorescent images of CDCP1 and E-Cadherin expression in salivary glands of the indicated genotypes. Scale bar represents 100 mm length. (C) Representative images of extra machrochaetae formation in adult fly notum expressing hCDCP1-WT or hCDCP1-delta or LacZ Control. Scale bar represents 100 mm length. (D) Representative images of macrochaetae formation in adult fly notum in heterozygous Src kinase mutant animals (src42A+/-; src64B+/-) or heterozygous Src kinase mutant animals are expressing hCDCP1-WT (src42A+/-; src64B+/-, CDCP1-WT). Scale bar represents 100 mm length.

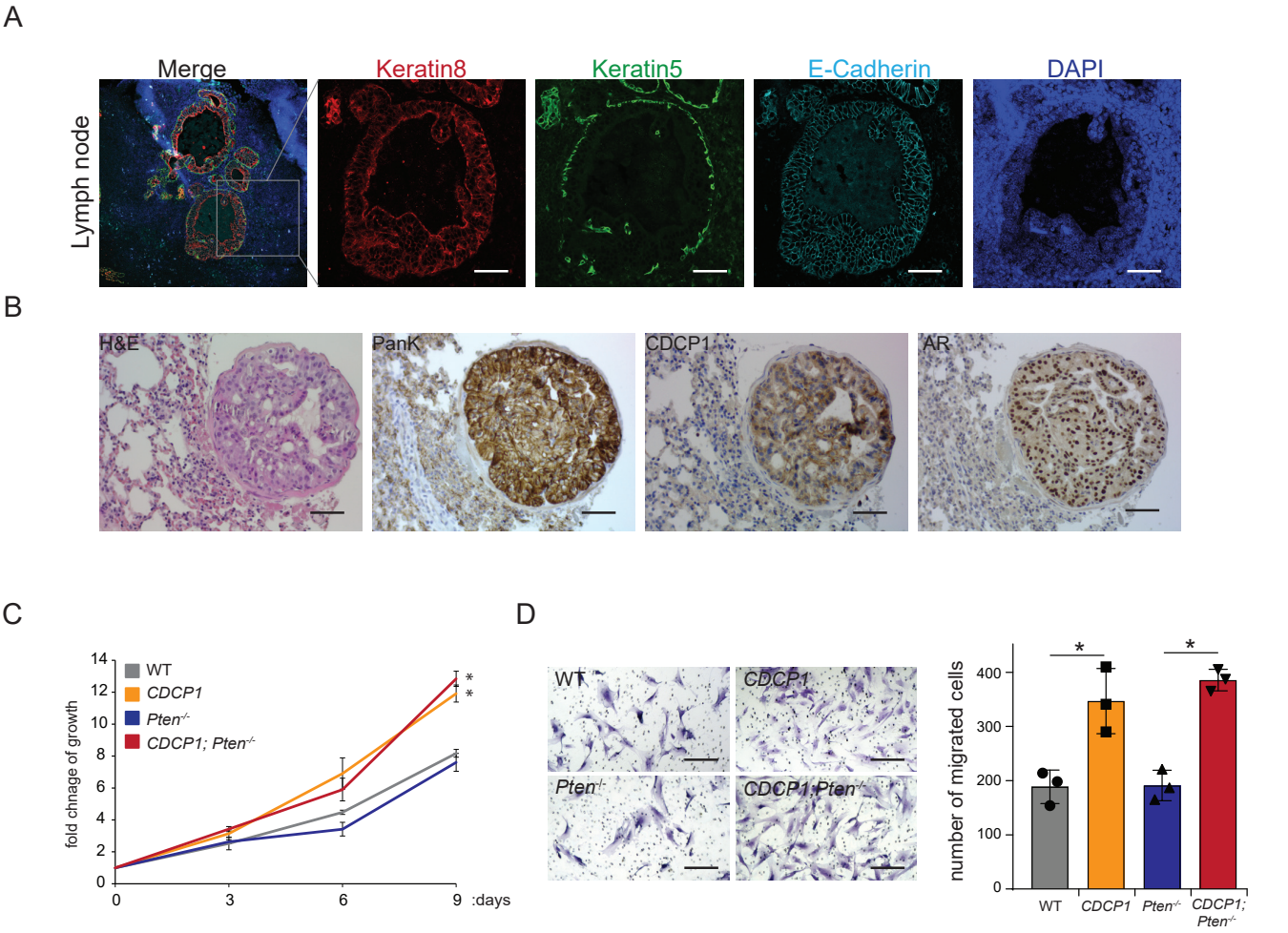

Supplementary Figure 4. CDCP1 overexpression in Pten-null tumours promotes a metastatic phenotype.
(A) Representative immunofluorescence staining of Keratin8, Keratin5, E-Cadherin and DAPI in lumbar lymph nodes from 10 months old *CDCP1; Pten*$^{pc-/-}$ mice. Insets represent higher magnification (scale bar 50 µm) (n=4/8). Scale bar represents 5 mm length. (B) Representative images of H&E, PanK, CDCP1 and AR staining in lungs from 10 months old *CDCP1; Pten*$^{pc-/-}$ mice (n=1/10). Scale bar represents 5 mm length. (C) Growth curve estimated by crystal violet staining in WT, *CDCP1, Pten*$^{-/-}$ and *CDCP1; Pten*$^{-/-}$ MEFs (n=3). (D) Left panel, Repre sentatives images of the trans-well migration assay in WT, *CDCP1, Pten*$^{-/-}$ and *CDCP1; Pten*$^{-/-}$ MEFs. Scale bar represents 5 mm length. Right panel, quantification of the migrated cells (n=3). Error bars indicate standard deviation (SD). *P<0.05. Statistic test used: two-tailed t-test.

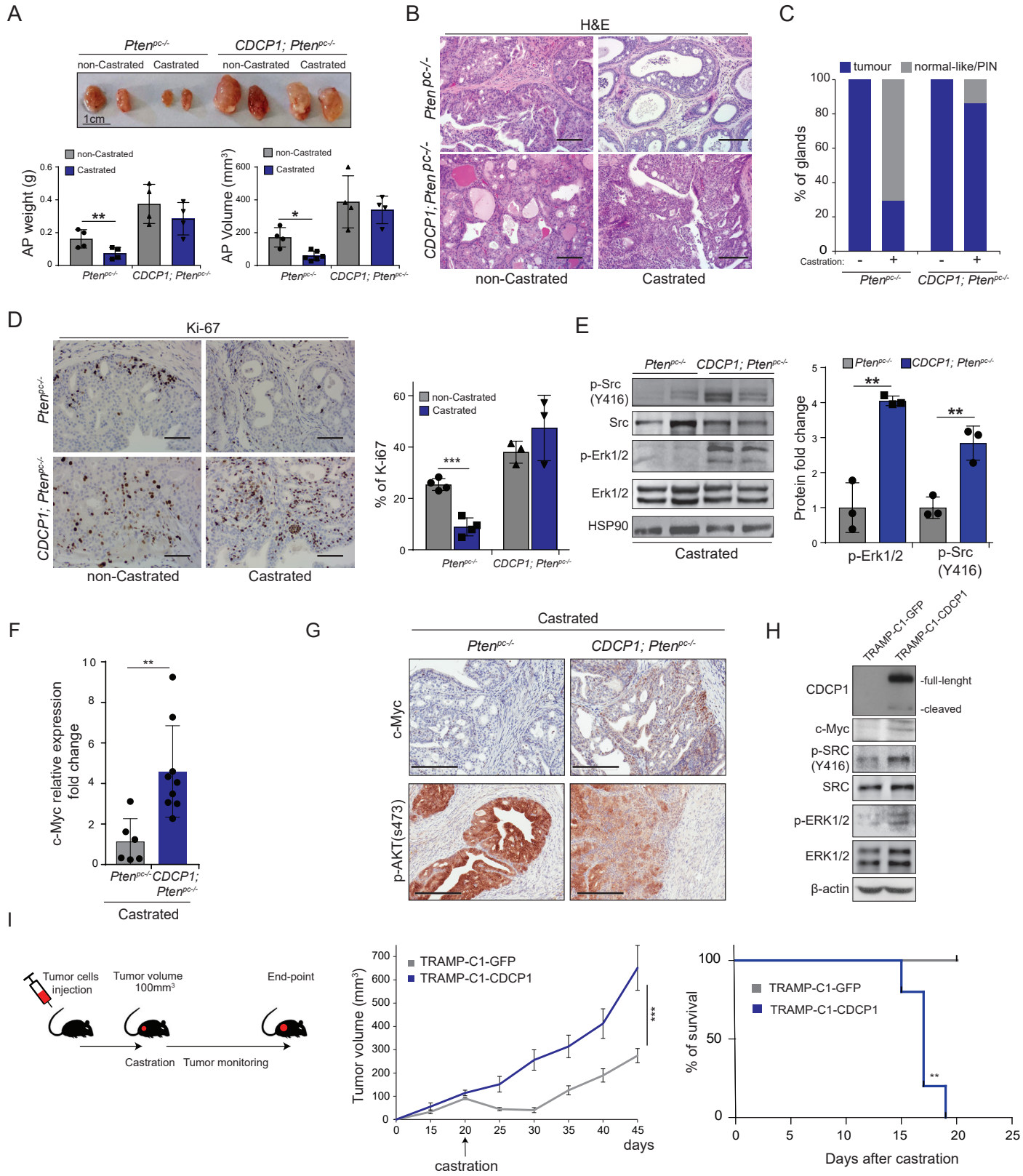

Supplementary Figure 5. CDCP1 overexpression in Pten-loss context leads to castration resistant prostate cancer
(A) Upper panel, representative images of anterior prostate of Pten$^{pc-/-}$ and CDCP1; Pten$^{pc-/-}$ non-castrated and castrated animals. Scale 1 cm. Lower panel, Quantification of anterior prostate weights and volume of Pten$^{pc-/-}$ and CDCP1; Pten$^{pc-/-}$ castrated and non-castrated mice (n=4). (B) Representatives images of H&E staining of Pten$^{pc-/-}$ and CDCP1; Pten$^{pc-/-}$ anterior prostate of non-castrated and castrated mice. All mice were sacrificed at the age of 20 weeks, 8 weeks after castration. Scale bar represents 5 mm length. (C) Quantification of histopathological markers from anterior prostate tissue of the indicated genotypes of Pten$^{pc-/-}$ and CDCP1; Pten$^{pc-/-}$ castrated and non-castrated mice (n=3). (D) Left panel, Representatives images of KI67 staining of Pten$^{pc-/-}$ and CDCP1; Pten$^{pc-/-}$ anterior prostate of non-castrated and castrated mice. Scale bar represents 5 mm length. Right panel, Quantification of Ki-67 staining in Pten$^{pc-/-}$ and CDCP1; Pten$^{pc-/-}$ anterior prostate of non-castrated and castrated mice at 20 weeks of age (n=3-4). (E) Western blot analysis and protein fold change quantification of indicated protein in the anterior prostate of Pten$^{pc-/-}$ and CDCP1; Pten$^{pc-/-}$ castrated mice at 20 weeks of age. (F) c-Myc relative expression fold change in Pten$^{pc-/-}$ and CDCP1; Pten$^{pc-/-}$ castrated mice. (G) Representative image of IHC staining of c-Myc and p-AKT (s473) in Pten$^{pc-/-}$ and CDCP1; Pten$^{pc-/-}$ castrated mice. Scale bar represents 200 mm. (H) Western blot analysis of CDCP1, c-Myc, p-Src, Src, p-Erk1/2 and Erk1/2 in TRAMP-C1-GFP and TRAMP-C1-CDCP1 mouse prostate cancer cell lines. (I) Left panel, representative scheme of TRAMP-C1 allograft experiment. Middle panel, Allograft tumors volume (mm^3) of TRAMP-C1-GFP and TRAMP-C1-CDCP1 cells. (n=5 in both groups). Right panel, Percentage of cumulative survival of TRAMP-C1-GFP and TRAMP-C1-CDCP1 allografts. Error bars indicate standard deviation (SD). **P<0.01; ***P<0.001. Statistic test used: two-tailed t-test for panel A, D, E and F. log-rank (mantel-cox) test for panel I.

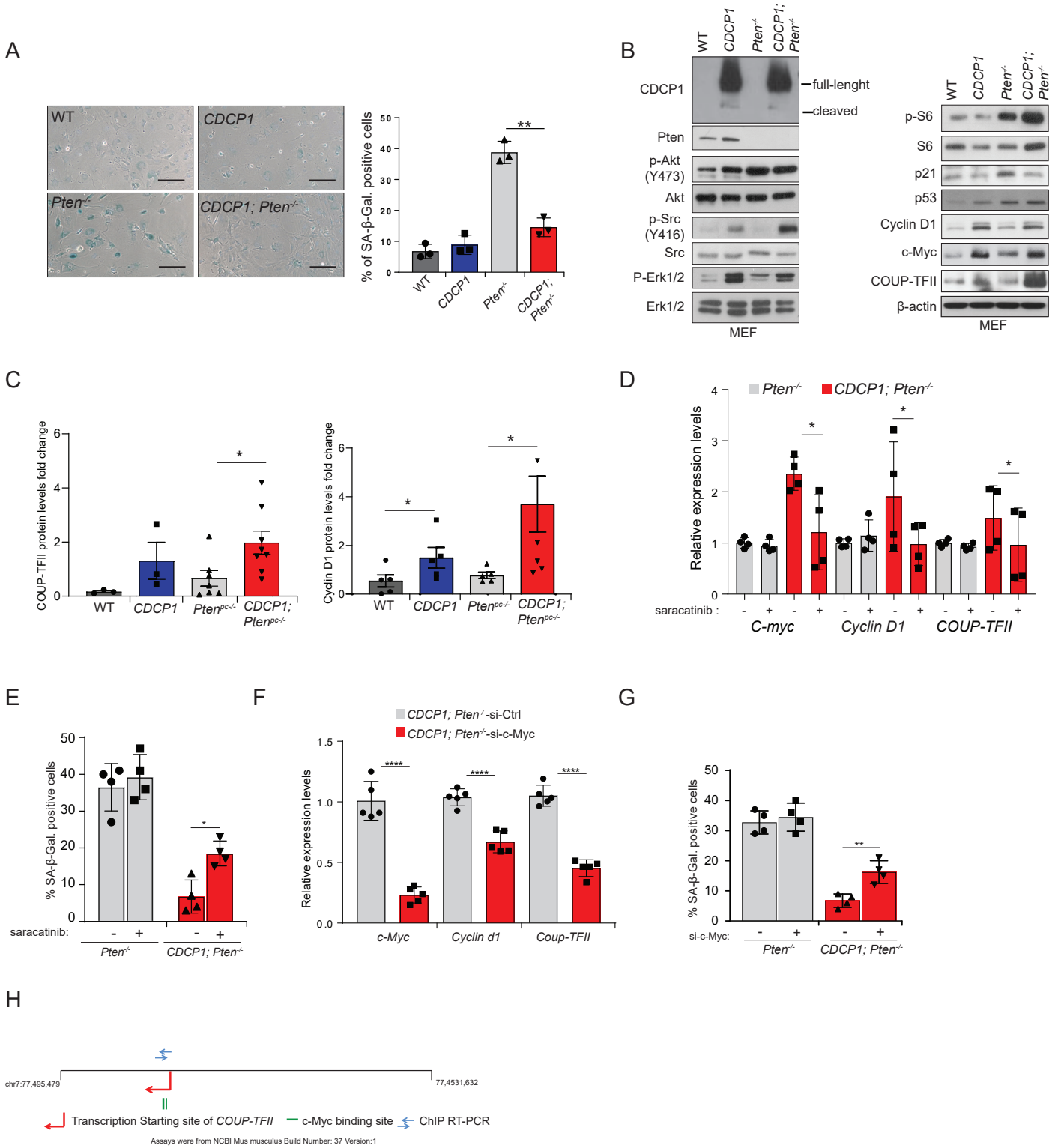

Supplementary Figure 6. CDCP1 overexpression promotes the escape from senescence in MEFs
(A) Representative images and quantification of SA-β-Gal staining in WT, *CDCP1, Pten*$^{-/-}$ and *CDCP1; Pten*$^{-/-}$ MEFs (n=3). Scale bar represents 5 mm length. (B) Western blot analysis of indicated proteins in WT, *CDCP1, Pten*$^{-/-}$ and *CDCP1; Pten*$^{-/-}$ MEFs. (C) Protein fold change uantification of COUP-TFII and Cyclin D1. (D) Quantitative real-time PCR analysis of c-Myc, Cyclin D1 and COUP-TF-II expression in *Pten*$^{-/-}$ and *CDCP1; Pten*$^{-/-}$ MEFs treated with saracatinib (100 nM) for 12 h (n=4). (E) Quantification of SA-β-Gal positive cells in *Pten*$^{-/-}$ and *CDCP1; Pten*$^{-/-}$ MEFs treated with saracatinib (100 nM) and DMSO for 12h (n=4). (F) Quantitative real-time PCR analysis of c-Myc, Cyclin D1 and COUP-TF-II expression in *Pten*$^{-/-}$ and *CDCP1; Pten*$^{-/-}$ MEFs transfected with si-c-Myc and control si-Ctrl after 48h (n=5). (G) Quantification of senescence-associated β-Gal (SA-β-Gal) staining in *Pten*$^{-/-}$ and *CDCP1; Pten*$^{-/-}$ MEFs transfected with si-c-Myc and control si-Ctrl after 48h (n=4). (H) Schematic representation showing the transcription starting site of COUP-TFII and c-Myc binding site (http://www.sabiosciences.com). Error bars indicate standard deviation (SD) for panels A, D, E, F and G and standard error mean (SEM) for panel C. *P<0.05; **P<0.01; ****P<0.0001. The following statistical tests were used: unpaired two-tailed t-test for panel A, D, E, F and G and one-tailed t-test for panel C.

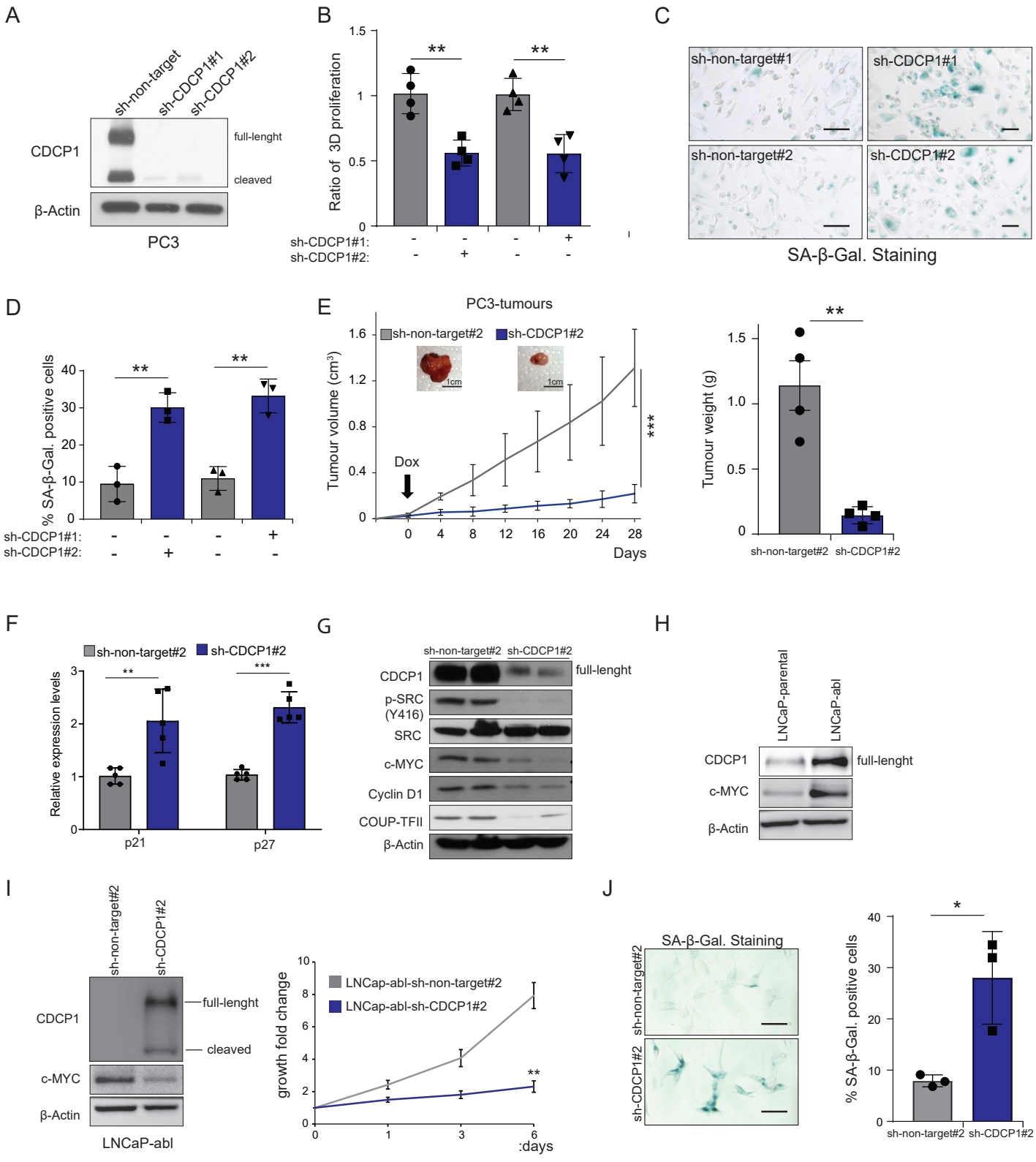

Supplementary Figure 7. CDCP1 overexpression promotes escape from senescence in human prostate cancer cell lines
(A) Western blot analysis of the CDCP1 protein in infected PC3 cells expressing PLKO-sh-CDCP1 (sh-CDCP1#1) and doxycycline-inducible Tripz-sh-CDCP1 (sh-CDCP1#2). (B) Quantification of in vitro 3D growth of CDCP1 depleted PC3 cells and control as measured by Luminescent Cell Viability Assay (n=4). (C) Representative image of SA-β-Gal staining of CDCP1 depleted PC3 cells and control PC3. Scale bar represents 5 mm length. (D) Bar graph represents the percentage of SA-β-Gal positive cells in all groups (n=3). (E) Left panel, Xenograft tumor growth (cm^3) of PC3 cells expressing doxycycline-inducible shRNA-control (sh-Ctrl#2) and shRNA-CDCP1 (sh-CDCP1#2). Insets represent PC3 xenograft tumors for both groups. Scale 1 cm. Right panel, bar graph represents tumor weight in both groups (n=4). (F) qRT-PCR of p27 and p21 mRNA levels in PC3 sh-Ctrl#2 and PC3 sh-CDCP1#2 xenografts tumors (n=4). (G) Western blot analysis of CDCP1, p-SRC, SRC, c-MYC, CYCLIN D1, COUP-TFII in PC3 sh-Ctrl#2 and PC3 sh-CDCP1#2 xenografts tumor. (H) Western blot analysis of CDCP1 and c-MYC in androgen deprivation sensitive LNCaP (LNCaP-parental) and androgen deprivation insensitive LNCaP-abl human prostate cancer cell line. (I) Left panel, Western blot analysis of CDCP1 and c-MYC in LNCaP-abl-shCtrl#2 and LNCaP-sh-CDCP1#2. Right panel, Fold change in growth of LNCaP-abl-shCtrl#2 and LNCaP-sh-CDCP1#2 (n=3). (J) Left panel, Representative images of SA-β-Gal staining in LNCaP-abl expression sh-Ctrl#2 and sh-CDCP1#2. Scale bar represents 5 mm length. Right panel, bar graph represents the percentage of SA-β-Gal positive cells in LNCaP-abl expression sh-Ctrl#2 and sh-CDCP1#2. (n=3). Error bars indicate standard deviation (SD). *P<0.05; **P<0.01; ***P<0.001. Statistic test used: two-tailed t-test.

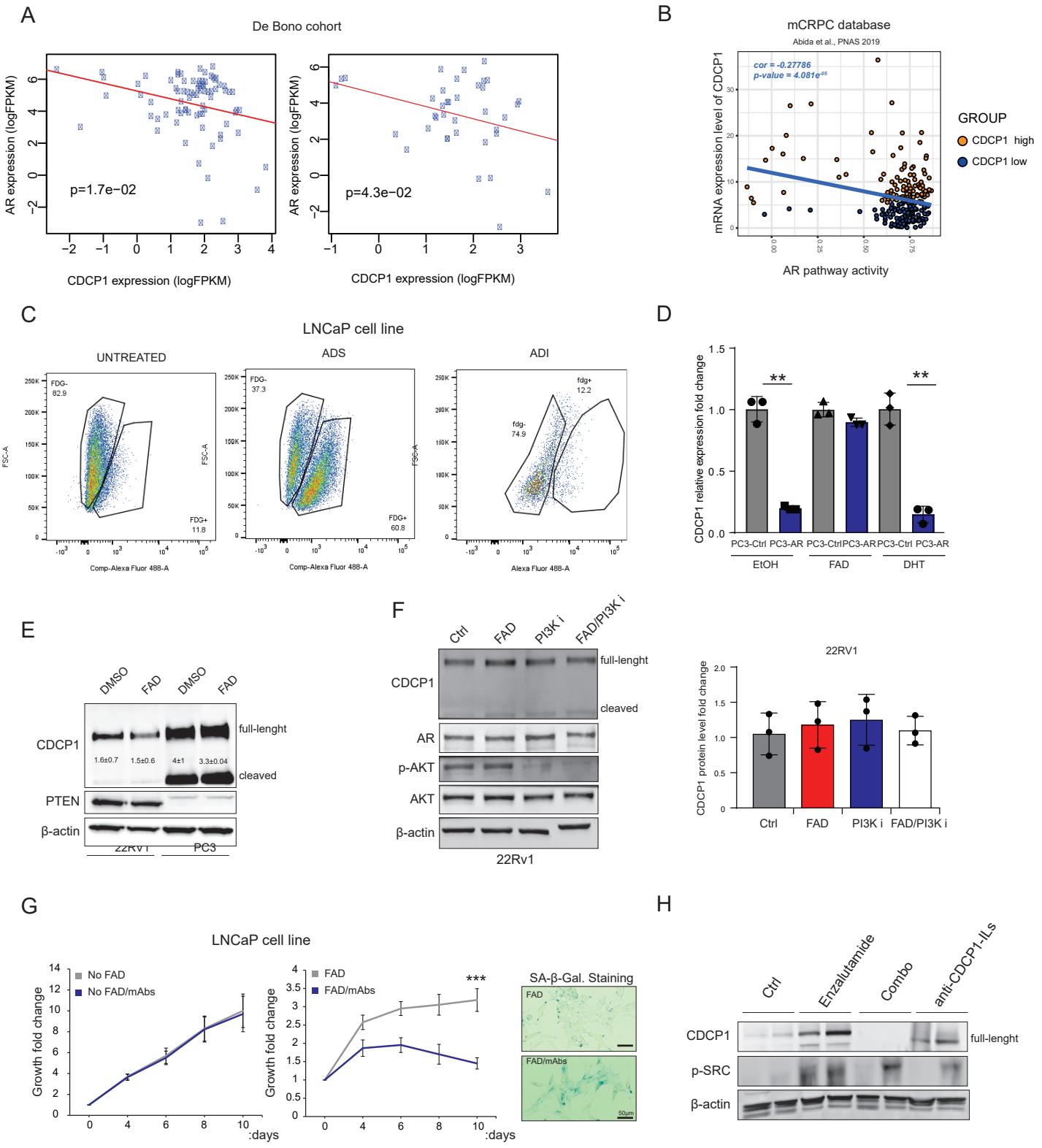

Supplementary Figure 8. CDCP1 expression is regulated by AR activity
(A) Left panel, negative correlation between CDCP1 expression levels and AR expression levels in the cases with PTEN expression low. Right panel, negative correlation between CDCP1 expression levels and AR expression levels in the cases with AR gene copy number normal. (B) Negative correlation between mRNA expression levels of CDCP1 with AR pathway activity (single sample GSEA score). (C) Dot-plots showing FDG staining in LNCaP cells untreated, LNCaP ADS and ADI. (D) Quantitative real-time PCR analysis of CDCP1 mRNA levels in PC3 and PC3-AR kept in full media, in FAD or under DHT stimulation (n=3) . (E) Western blot analysis of CDCP1 and PTEN in androgen insensitive human prostate cancer cell lines (22RV1 and PC3) (n=3). (F) Left panel, Western blot analysis of CDCP1, AR, p-AKT and AKT in 22RV1 treated with PI3K inhibitor in normal condition and in FAD. Right panel, Quantification of fold change in CDCP1 protein levels in 22RV1 untreated or treated with PI3K inhibitor in normal condition and in FAD (n=3). (G) Left panel, Quantification of fold change in growth by crystal violet in LNCaP kept in full media and FAD and treated with and without the mAb-CUB4. Right panel, SA-b-Gal staining in cells treated with the indicated antibody. Scale bar represents 50 μm. (H) Western blot analysis of CDCP1 expression and p-SRC in LNCaP xenografts groups. Error bars indicate standard deviation (SD). **P<0.01; ***P<0.001. Statistic test used: two-tailed t-test.